Chinese Chemical Letters 34 (2023) 107863

Contents lists available at ScienceDirect

Chinese Chemical Letters

journal homepage: www.elsevier.com/locate/cclet

Construction of nanoreactors on TiO_2 nanotube arrays as a POCT device for sensitive colorimetric detection

Jingwen Xu, Chenchen Liang, Zhida Gao, Yan-Yan Song*

College of Sciences, Northeastern University, Shenyang 110004, China

ARTICLE INFO

Article history:
Received 8 June 2022
Revised 13 September 2022
Accepted 26 September 2022
Available online 29 September 2022

Keywords:
Point-of-care testing
TiO_2 nanotube arrays
Colorimetry
Alkaline phosphatase
Nano test tube

ABSTRACT

With increasing attention to personalized healthcare, miniaturized and easily implementable devices are desired for point-of-care testing (POCT). Herein, hydrophilic patterns were designed on freestanding TiO_2 nanotube arrays (TiNTs) as nanoreactors for a naked-eye colorimetric assay. With a high aspect ratio, TiNTs can provide a long observation length combined with a limited volume. Moreover, by combining the photocatalytic property of TiO_2 and spatiotemporal controllability of light, hydrophilic nanoreactors were fabricated with minimal volume, and thus the indicator and analyte are limited in a confined void by the hydrophobic surroundings, thus allowing a higher sensitivity for sensing. We believe the proposed sensing platform could provide a promising strategy in developing POCT devices for routine health monitoring.

Point-of-care testing (POCT) technologies have attracted much attention owing to their potential to avoid complex laboratory operations and enable routine health monitoring [1–4]. With the current demand of personalized healthcare and home diagnosis, it is desired to develop POCT devices with the characteristics of simple operation, effective signal amplification, and portability for biomarker detection [5–8]. Miniaturized POCT devices have been recently developed, where electrochemistry [9,10], fluorescence [11,12], and microfluidics [13,14] were widely used owing to their low cost and rapid diagnosis. However, these methods require extra devices such as an electrochemical workstation, excitation light source, or injection pump, thus increasing the operation difficulty. Thus, they cannot satisfy the demand of easy-to-use devices for home diagnosis. Colorimetric assay can provide a power-free and straightforward readout signal by simple color changes, thus offering a solution for easy-to-use POCT devices [5,15,16].

Porous materials have been extensively developed as substrates for colorimetric assay, as their large specific surface area can provide abundant sites for probe molecule immobilization and analyte enrichment [17,18]. In recent years, TiO_2 nanotube arrays (TiNTs) have attracted much interest ranging from drug delivery to biosensing owing to their intrinsic photocatalytic activity, high surface-to-volume ratio, and perpendicular structure to the substrate surface, and the presence of functional groups such as OH group on their surface [19–25]. Because TiNTs prepared by electrochemical anodization are readily adjustable in morphology (pore sizes, and aspect ratio), optical property, and surface charge, TiNTs can provide a flexible scaffold to load biomolecules or indicators for biosensing and optical detection [26–30]. Furthermore, amphiphilic nanotubes can be designed by utilizing the photocatalytic activity of TiO_2 [31,32], thus allowing distinct regions in one substrate and expanding the functionality of TiNTs.

In this study, we designed hydrophilic patterns on TiNTs as nanoreactors for a highly sensitive naked-eye colorimetric assay. The fabrication procedure is shown in Fig. 1. In this design, TiNTs with a high aspect ratio and perpendicular arrays were grown with an electrochemical anodization and then removed from a Ti substrate to obtain a freestanding membrane. Then, the surface wettability of TiNTs was adjusted by coating a layer of hydrophobic molecules. By utilizing the photocatalytic activity of TiO_2, hydrophilic patterns with a hydrophobic surrounding were fabricated on TiNTs *via* simple UV irradiation with aid of a mask. These small-sized hydrophilic compartments were then used as nanoreactors for colorimetric assay. As a proof-of-concept, alkaline phosphatase (ALP), an essential enzyme that relates to the dephosphorization of important life processes, was used as the model analyte to demonstrate the use of the proposed sensing platform. The detection mechanism is shown in Fig. 1. Hydrophilic nanoreactors were functionalized and loaded with indicators zincon-Zn(II) chelates (ZC-Zn(II)). As an enzyme substrate of ALP, pyrophosphate (PPi) can be hydrolyzed by ALP to phosphate ions (Pi). Moreover, the affinity of Zn(II) to zincon is stronger than Pi and weaker than PPi. There-

* Corresponding author.
E-mail address: yysong@mail.neu.edu.cn (Y.-Y. Song).

https://doi.org/10.1016/j.cclet.2022.107863
1001-8417/

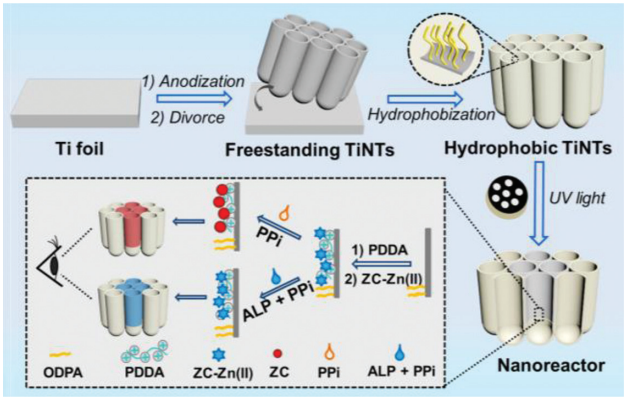

Fig. 1. Schematic diagram for the preparation of hydrophilic nanoreactors on TiNTs and detection mechanism of colorimetric analysis of ALP.

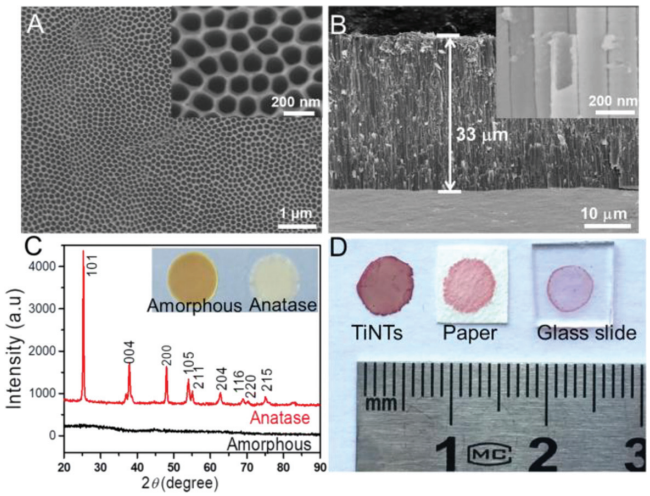

Fig. 2. SEM images of (A) top side and (B) cross-sectional side of TiNTs. (C) XRD patterns and digital images of amorphous and anatase TiNTs. (D) Comparison of colorimetric performance: 10 μL of zincon (0.05 g/L) dripped onto TiNTs, paper, and glass slide.

fore, the presence of PPi can trigger the release of red-colored zincon by competitive coordination of PPi-Zn(II), while blue-colored ZC-Zn(II) is insusceptible in the presence of Pi. Based on the distinct color responses, the proposed platform can provide a straightforward readout signal for ALP colorimetric assay.

TiNTs used in this study were prepared by electrochemical anodization in a NH_4F-containing organic electrolyte. Scanning electron microscopy (SEM) images in Figs. 2A and B show that the as-prepared TiO_2 nanotubes have a uniform porous nanostructure with a diameter of 150 ± 20 nm and length of ~33 μm, and TiNTs are composed of numerous perpendicular nanotubes with closed tube bottom (Fig. S1 in Supporting information). The specific Brunauer-Emmett-Teller (BET) surface areas of TiO_2 NTs was determined as 47.459 m^2/g (Fig. S2 in Supporting information), indicating the high specific surface area of TiNTs. To achieve high chemical stability, the TiNTs were annealed at 450 °C in air for 2 h. As most of the contamination inside TiNTs can be burnt off by high-temperature calcination, the color of TiNTs transferred to a pale yellow (Fig. 2C inset), which can offer a low background for naked-eye colorimetric assay. The X-ray diffraction (XRD) pattern in Fig. 2C shows specific diffraction peaks of anatase after the annealing treatment, suggesting the successful transfer from amorphous TiO_2 to anatase. Compared with amorphous TiO_2, anatase has a higher chemical stability and photocatalytic activity, which is beneficial for the fabrication of hydrophilic reactors on TiNTs. The

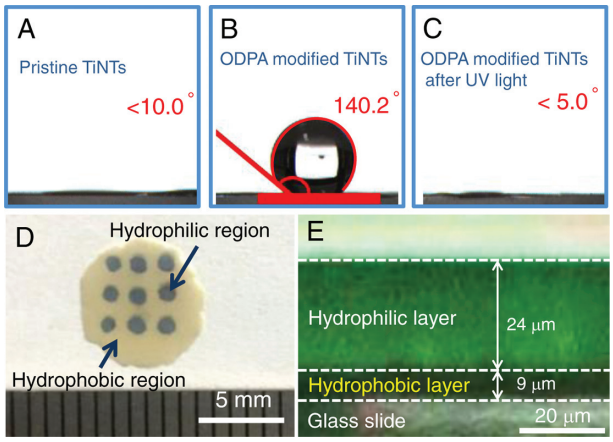

Fig. 3. Images of water droplets on (A) pristine TiNTs, (B) hydrophobic TiNTs, and (C) hydrophobic TiNTs after UV irradiation. (D) Digital image of TiNTs with blue-colored indicator in hydrophilic arrays. (E) Cross-sectional fluorescence image of TiNTs with a hydrophilic reactor.

colorimetric performance of TiNTs was then evaluated by adding the same volume of red-colored indicator (zincon, zinc metal-organic complex) to the glass slide, filter paper, and TiNTs. As expected, a much higher red-color intensity can be observed from TiNTs than other substrates (Fig. 2D). The large surface area of TiNTs offers a plenty of available sites for indicator attachment, while the nano test tube structure of TiNTs with a high aspect ratio can provide a long observation length combined with a limited volume. Therefore, TiNTs can amplify the optical signal and thus exhibit an excellent colorimetric performance.

By utilizing the intrinsic photocatalysis activity of TiO_2, distinct hydrophilic/hydrophobic regions were fabricated on TiNTs to form small-sized nanoreactors to further improve the colorimetric performance. As pristine TiNTs showed a hydrophilic surface (Fig. 3A), a hydrophobic monolayer, octadecylphosphonic acid (ODPA), was coated on TiNTs, and the surface was converted to hydrophobic with a water contact angle of 140.2° (Fig. 3B). With abundant surface active sites in anodized TiNTs, hydrophobic ODPA was modified onto the nanotube *via* affinity interaction between the Ti-OH and phosphonic acid [33]. Then, the wettability of TiNTs was further adjusted by the decomposition of hydrophobic chains induced by the photocatalysis of TiO_2 under UV irradiation. As shown in Fig. 3C, the water contact angle decreased to <5° after being exposed to UV light for a short time, suggesting the full degradation of hydrophobic chains on TiNTs. According to the abovementioned results, patterned hydrophilic regions were formed on hydrophobic TiNTs by covering a mask with open areas. Fig. 3D shows the digital image of patterned hydrophilic regions with a diameter of 1.0 mm on TiNTs. Because of the coverage of a patterned mask, photodegradation of hydrophobic chains is confined to areas exposed to UV light, while the hydrophobic chains in shadowed areas are reserved. With the hydrophobic surrounding, the blue indicators are well held in hydrophilic regions without spreading. Fig. 3E shows the cross-section fluorescent image of sodium fluorescein loaded hydrophilic compartments. With the limited transparent depth of UV light, the thickness of hydrophilic layer was ~24 μm, while the bottom of nanotubes exhibited a dark color without wetting by sodium fluorescein. Therefore, the volume of one hydrophilic compartment was calculated as 18.8 nL. These hydrophilic compartments with such a tight volume acted as nanoreactors, which can limit the indicators and analyte in a confined void, enabling the colorimetric assay with a high sensitivity.

To demonstrate the use of TiNTs for specific and sensitive analysis of disease-related biomarkers, we studied the detection of ALP

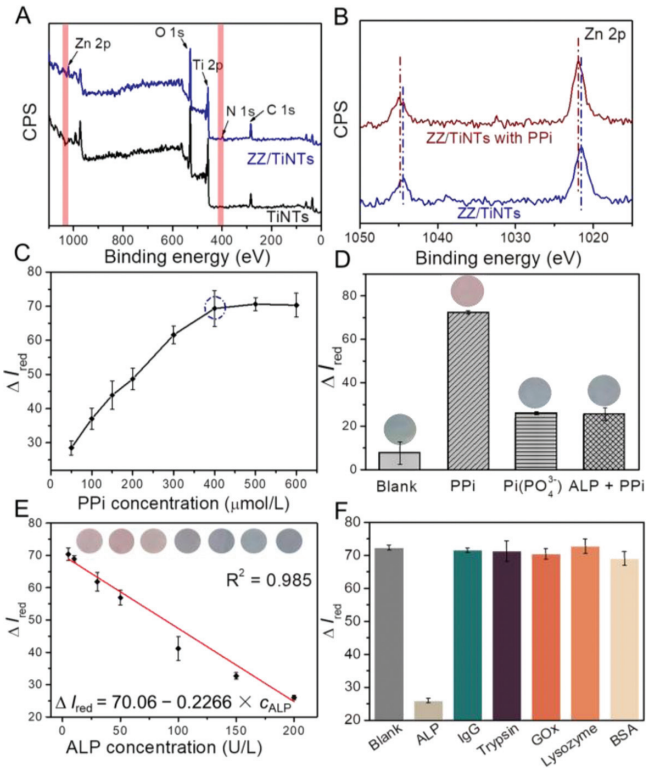

Fig. 4. (A) Survey XPS spectra of TiNTs and ZZ/TiNTs. (B) Zn 2p signals for ZZ/TiNTs and ZZ/TiNTs with PPi. CPS: counts per second. (C) ΔI_{red} responses of ZZ/TiNTs to PPi with different concentrations. (D) ΔI_{red} responses of ZZ/TiNTs to buffer solution, PPi, Pi(PO_4^{3-}), and a mixture of PPi and ALP. (E) ΔI_{red} *versus* ALP activity from 2 U/L to 200 U/L. (F) ΔI_{red} responses of ZZ/TiNTs to ALP (200 U/L) and interfering proteins (10 mmol/L).

using the proposed TiNTs in a colorimetric assay. First, the TiNTs were coated with a layer of poly(diallyldimethylammonium chloride) (PDDA), and thus abundant binding sites can be provided by the amino groups in PDDA for the grafting of negatively charged indicators *via* electrostatic interaction. The successful decoration of PDDA was confirmed by the positive shift of zeta potential from −24.7 mV to 33.9 mV (Fig. S3 in Supporting information). Then, blue-colored zincon-Zn(II) chelates (ZC-Zn(II)) as indicators were loaded by immersing bare TiNTs into a solution containing ZC-Zn(II) after an incubation time of 35 min (Fig. S4 in Supporting information), and the substrate showed a blue color in hydrophilic nanoreactors (Fig. 3D). This step was then confirmed by X-ray photoelectron spectroscopy (XPS). As shown in Fig. 4A, the peaks of Zn 2p and N 1s appeared after the loading of ZC-Zn(II), while decreased intensities of Ti 2p and O 1s peaks can be attributed to the coverage of ZC-Zn(II) on the surface of TiO_2. As the ALP activity is evaluated by its hydrolysis towards PPi, the response of ZC-Zn(II) to PPi is crucial for colorimetric assay. As shown in Fig. 4B and Fig. S5 (Supporting information), the XPS peaks of Zn 2p showed a distinct shift to a higher energy in the presence of PPi. Because of the higher affinity between PPi and Zn^{2+} ions, ZC-Zn(II) were substituted by the competitive coordination of PPi-Zn(II) framework, thus resulting in a higher binding energy of Zn 2p. Effect of PPi concentrations to the color change of ZC-Zn(II) chelate loaded TiNTs (ZZ/TiNTs) was further evaluated [34,35]. To provide a more accurate quantification of color variation, distribution of the red parameter of the Red-Green-Blue (RGB) system was analyzed using image J software, and the color variation of ZZ/TiNTs was quantified from the intensity difference of red parameter (ΔI_{red}, calculated as $I - I_0$, where I_0 and I represent the intensities of red parameter of substrate before and after testing). As shown in Fig. 4C, ΔI_{red} of ZZ/TiNTs continuously increased with increasing PPi concentration, while ΔI_{red} became stable when the PPi concentration was more than 400 μmol/L. Hence, the PPi concentration in colorimetric assay was selected as 400 μmol/L, because excessive PPi will consume ALP and reduce the sensitivity of detection. As PPi can be hydrolyzed by ALP to Pi ($H_2PO_4^-$, HPO_4^{2-}, or PO_4^{3-}), the feasibility of the sensing platform for ALP assay was validated by evaluating the color changes of ZZ/TiNTs in the presence of PPi, Pi(PO_4^{3-}), and hydrolysis product of PPi and ALP. As shown in Fig. 4D, ZZ/TiNTs incubated with PPi exhibited a high ΔI_{red} of 72.4, which is much higher than that obtained with a mixture of ALP and PPi or only Pi. In the presence of PPi, the ZC-Zn(II) chelate was cleaved by the competitive coordination of PPi-Zn(II) framework, and thus unpaired ZC remained on the surface of TiNTs, exhibiting a red color. Compared with PPi, Pi showed a quite low affinity towards Zn^{2+} ions, and thus no distinct color change can be observed from ZZ/TiNTs. With an incubation time of 60 min (Fig. S6 in Supporting information), PPi can be hydrolyzed by ALP to Pi thoroughly. Based on this hydrolysis, a mixture of ALP and PPi was incubated at 37 °C for 60 min, followed by immersing ZZ/TiNTs in the resulting solution. As a result, a negligible color change can be observed from ZZ/TiNTs, indicating the maintenance of ZC-Zn(II) in TiNTs.

The analytical performance of the proposed sensing platform was then evaluated using ALP solution at a clinically relevant concentration range. Prior to detection, the colorimetric assay was evaluated by varying the reaction time from 5 min to 30 min (Fig. S7A in Supporting information), and pH from 2.5 to 11.5 (Fig. S7B in Supporting information). The optimal reaction time and pH are 15 min and 8.5, respectively. Based on the calibration curve plotted in Fig. 4E, the ΔI_{red} of ZZ/TiNTs displayed a good linear profile from 2 U/L to 200 U/L, with the square of linear correlation coefficient (R^2) of 0.985. The limit of detection (LOD) was estimated to be 1 U/L ($3\sigma/s$, where σ is the standard deviation of the blank, and s is the slope of the calibration plot). Furthermore, the selectivity of the proposed sensing platform towards ALP is shown in Fig. 4F in the presence of several potential interferences including immunoglobulin G (IgG), trypsin, glucose oxidase (GOx), lysozyme, and bovine serum albumin (BSA). Compared with the high ΔI_{red} value of ZZ/TiNTs loaded with only PPi (blank), the presence of ALP can lead to a clear decrease of ΔI_{red} value, while the presence of other interfering proteins would not trigger the decrease of ΔI_{red} value. These interfering proteins did not influence the decomposition of ZC-Zn(II) stimulated by PPi, consistent with the specific hydrolytic ability of ALP towards PPi. The reusability of the proposed sensing platform was investigated by refreshing in a Zn(II) containing solution after ALP detection. The I_{red} values for ALP sensing and after the refreshed treatment were recorded in Fig. S8A (Supporting information). In five cycles, the same sample showed satisfactory repeatability. Moreover, the sensing platform showed a good stability after storage in air for 10 days (Fig. S8B in Supporting information).

A practical application of the sensing platform was performed using diluted human serum samples with the addition of standard concentrations of ALP. The prepared spiked serum samples with additional ALP and PPi were first incubated at 37 °C for 60 min, and then ZZ/TiNTs were dipped in this solution for another 15 min to measure the color changes. The results in Table S1 (Supporting information) showed that the recoveries of ALP in diluted serum samples are in the range of 103.5%−107.7%. Compared to the commercial ALP ELISA kit, no significant difference was observed. Therefore, this sensing system was found to be suitable for the qualitative analysis of ALP in a complex biological sample with good recovery and precision.

In conclusion, we have successfully developed a naked-eye colorimetric sensing platform based on a freestanding TiNTs mem-

brane. The high aspect ratio and perpendicular TiO_2 nano test tubes in TiNTs provided a long observation length for colorimetric assay. By combining the photocatalysis property of TiO_2 and surface functionalization strategy, hydrophilic compartments with a minimal volume were designed on TiNTs as nanoreactors, which can limit indicators and analyst in a confined void, thus improving the sensitivity. ALP concentrations ranging from 2 U/L to 200 U/L can be detected by the proposed colorimetric sensing platform with a high selectivity against other proteins and biological species. The proposed TiNT-based sensing platform paves a new way for constructing a miniaturized and easily implementable POCT device for the monitoring of routine biomarkers.

Declaration of competing interest

The authors declare that they have no known competing financial interests or personal relationships that could have appeared to influence the work reported in this paper.

Acknowledgments

We acknowledge the financial support from the National Natural Science Foundation of China (Nos. 21874013, 22204016 and 22074013), and the Fundamental Research Funds for the Central Universities (Nos. N2005027, N2105018, and N2205005).

Supplementary materials

Supplementary material associated with this article can be found, in the online version, at doi:10.1016/j.cclet.2022.107863.

References

[1] M. Alafeef, P. Moitra, K. Dighe, D. Pan, Nat. Protoc. 16 (2021) 3141–3162.
[2] J. Wang, C. Jiang, J. Jin, et al., Angew. Chem. Int. Ed. 60 (2021) 13042–13049.
[3] C. Wang, M. Liu, Z. Wang, et al., Nano Today 37 (2021) 101092.
[4] J. Dai, H. Zhang, C. Huang, Z. Chen, A. Han, Anal. Chem. 92 (2020) 16122–16129.
[5] Y. Xu, T. Wang, Z. Chen, et al., Chin. Chem. Lett. 32 (2021) 3675–3686.
[6] B. Gao, Y. Yang, J. Liao, B. He, H. Liu, Lab Chip 19 (2019) 3602–3608.
[7] L. Zhi, S. Zhang, M. Li, J. Tu, X. Lu, ACS Appl. Mater. Interfaces 14 (2022) 9442–9453.
[8] Y. Wang, H. Lu, M. Guo, et al., Adv. Healthcare Mater. 11 (2022) 2101659.
[9] H. Gao, L. Wen, J. Tian, et al., Biosens. Bioelectron. 142 (2019) 111504.
[10] S. Boonkaew, I. Jang, E. Noviana, et al., Sensor. Actuator. B: Chem 330 (2021) 129336.
[11] S. Wang, M. Huang, J. Hua, et al., Nanoscale 13 (2021) 4946–4955.
[12] N.T. Thet, J. Mercer-Chalmers, R.J. Greenwood, et al., ACS Sens 5 (2020) 2652–2657.
[13] G.A. Akceoglu, Y. Saylan, F. Inci, Adv. Mater. Technol. 6 (2021) 2100049.
[14] Z. Zhang, P. Ma, R. Ahmed, et al., Adv. Mater. 34 (2022) 2103646.
[15] S.K. Biswas, S. Chatterjee, S. Bandyopadhyay, et al., ACS Sens. 6 (2021) 1077–1085.
[16] Y. Zhu, Y. Tian, T. Zheng, Chem. Commun. 58 (2022) 3771–3774.
[17] Z.Y. Han, H.K. Li, Q.Q. Zhu, R. Yuan, H. He, Chin. Chem. Lett. 32 (2021) 2865–2868.
[18] K. Qu, J. Xu, Y. Xue, et al., Anal. Chem. 94 (2022) 588–592.
[19] M.H. Zarifi, B. Wiltshire, N. Mahdi, et al., Nanoscale 10 (2018) 4882–4889.
[20] Z. Wu, I. Hwang, G. Cha, et al., Small 18 (2022) 2104892.
[21] L. Liang, J. Yin, J. Bao, et al., Chin. Chem. Lett. 30 (2019) 167–170.
[22] Y. Jia, P. Liu, Q. Wang, et al., J. Colloid Interf. Sci. 585 (2021) 459.
[23] Q. Wang, H. Li, X. Yu, et al., Electrochim. Acta 330 (2020) 135167.
[24] Q. Wang, S. Zhu, S. Zhao, et al., Fuel 322 (2022) 124163.
[25] Z. Liu, Y. Song, Q. Wang, et al., J. Colloid Interf. Sci. 556 (2019) 92–101.
[26] L. Yang, J. Feng, J.N. Wang, et al., Chin. Chem. Lett. 33 (2022) 5169–5173.
[27] Y.Y. Song, F. Schemidt-Stein, S. Berger, P. Schmuki, Small 6 (2010) 1180–1184.
[28] L.K. Dhandole, H.S. Chung, J. Ryu, J.S. Jang, ACS Sustain. Chem. Eng. 6 (2018) 16139–16150.
[29] G. Thomas, G. Gerer, L. Schlur, et al., Nanoscale 12 (2020) 13338–13345.
[30] N. Khaliq, M.A. Rasheed, M. Khan, et al., ACS Appl. Mater. Interfaces 13 (2021) 3653–3668.
[31] J. Xu, X. Zhou, Z. Gao, Y.Y. Song, P. Schmuki, Angew. Chem. Int. Ed. 55 (2016) 593–597.
[32] J. Zhao, J. Xu, X. Jian, et al., ACS Appl. Mater. Interfaces 12 (2020) 23606–23616.
[33] J. Guo, L. Yang, Z. Gao, et al., ACS Catal. 10 (2020) 5949–5958.
[34] C. Männel-Croisé, C. Meister, F. Zelder, Inorg. Chem. 49 (2010) 10220–10222.
[35] D.H. Lee, J.H. Im, S.U. Son, Y.K. Chung, J.I. Hong, J. Am. Chem. Soc. 125 (2003) 7752–7753.